Studying the Effect of Pulse Shape on Dynamic Stress Intensity Factor at the Finite Crack Tip using Displacement Fields

Hossein Rahmani *
Department of Mechanical Engineering,
University of Sistan and Baluchestan, Zahedan, Iran
E-mail: H_Rahmani@eng.usb.ac.ir
*Corresponding author

Mohammad Ahmadi Balootaki
Department of Mechanical Engineering,
University of Sistan and Baluchestan, Zahedan, Iran
Faculty of Shahid Bahonar, Sistan and Baluchestan Branch,
Technical and Vocational University (TVU), Zahedan, Iran
E-mail: M.Ahmadibalootaki@pgs.usb.ac.ir

Abstract: In analytical studies, step (Heaviside) function is used to simulate an impact load. However, in real behaviour of materials, loading and unloading take a short time. The present study discusses analytically the effects of pulse shape and rising time of an impact load on dynamic stress intensity factor. Firstly, a pulse load with positive slip (linear and non-linear) is applied on a cracked plate and the amount of dynamic stress intensity factor on the crack tip is obtained. Then the effects of pulse time are discussed. Results show that increasing the rise time decreases the stress intensity factor because of reduction of inertia effects. Moreover, the duration of rise time plays the main role in dynamic stress intensity factor changes and how the variations are not matter.

Biographical notes: Hossein Rahmani received his PhD in Mechanical Engineering from Semnan University in 2014. He is currently Assistant Professor at the Department of Mechanical Engineering, University of Sistan and Baluchestan, Zahedan, Iran. His current research interest includes impact engineering and elastodynamic. **Mohammad Ahmadi-Balootaki** is a PhD candidate of Mechanical Engineering at the University of Sistan and Baluchestan, Zahedan, Iran. He is currently lecturer at the Department of Mechanical Engineering, University of Sistan and Baluchestan, Zahedan, Iran and Faculty of Shahid Bahonar, Sistan and Baluchestan Branch, Technical and Vocational University (TVU), Zahedan, Iran. His current research focuses on mechatronics and control.

1 INTRODUCTION

Stress Intensity Factor (SIF), as one of the most important criteria in predicting the fracture behaviours of materials, has always attracted attentions of researchers. Fracture behaviours of materials under impact and dynamic loads are completely different from static mode. Inertia, reflection of stress waves, and the effects of the strain rate dependent behaviours of material are some differences between dynamic and static fracture behaviours. Therefore, calculating Dynamic Stress Intensity Factor (DSIF) is so complicated rather than SIF. Analytical methods, the finite element simulation, and the experimental tests are usually used for calculating DSIF. Sih was one of the first researchers who conducted an analytical study on the DSIFs of cracks and presented most basic methods for stress fields around crack tip and dynamic fracture [1]. Frund studied semi-infinite crack on unbounded body. He also studied DSIF on different fracture modes using step function. In this analysis, the equations, which were obtained using the dual Laplace transform, were simplified and solved using the Wiener-Hopf method [2]. Sih and Embely in one article and Stephen and Tsin-Hwei in another article discussed behaviour of crack analysis with a limited length on an unbounded body in a 2D mode. Using the Laplace transform from time domain and then Fourier sine and cosine transforms over space, they solved the wave equations and the fields created around a crack. The obtained dual integral equations were solved using the numerical methods and the value of DSIF around the crack was determined [3-4]. Yi-Shyoning and Chen-Chang Ma studied behaviour of the crack under anti-plane loading and obtained the value of DSIF for this type of waves at modes one and two [5]. In another study, they examined crack behaviour under the concentrated load imposed on a crack place under an anti-plane load [6]. The analytical equations of DSIF in orthotropic materials were obtained by Kassir and Bandyopadhyay. It was done for a cracked plate under distributed tension load [7]. Similarly, the analytical equations of DSIF in an orthotropic cracked plate under concentrated tension load were studied by Rubio-Ganzalez and Mason [8]. Rodriguez-Castellanos et al. discussed behaviour of DSIF using finite element method on a plate. In this study, the plate has a central crack and it is under an impact load. Here, the impact load was considered as a unit step function (Heaviside). After confirming the results obtained from the simulation method by using earlier practical studies, the effects of size and crack direction on distributing stress waves were examined [9]. Iotu solved the equations of DSIF for two cylindrical cracks in an unbounded elastic body under an impact load. The equations of stress and displacement boundary conditions were transformed to a system of dual integral equations using Laplace and the Fourier transforms. Then DSIF was determined in a Laplace environment. Finally, the results were returned to a place-time environment using the numerical methods. In this research, the impact load is considered as a Heaviside function [10]. Eslami and Amini studied the equations related to the stress fields at crack tip under the harmonic wave and obtained a relation to determine DSIF. In this research, the equations were initially transformed to a mixing environment by changing a variable and then they were solved [11]. Behaviour of stress wave pulse in penny-shape cracks was examined by Zhang using the Boundary Integral Method [12]. The boundary integral method is used in other researches for dynamic behaviour and crack analysis [13-16]. In the experimental methods, photo elasticity setups and strain gauges are usually used at crack tips to determine transient stress fields and dynamic stress intensity factor. Malezhik et al. studied determination of dynamic stress intensity factor using a photo elasticity unit. The sample under the test is made of composite and it is assumed that it remains at elastic state. In this research, an equation was obtained between stress fields at the points far from a crack tip and stress intensity factor [17]. In addition, several methods for DSIF calculating were discussed using the photo elasticity method and strain gauges [18].

For analytical solutions in reviewed articles, impact load is defined as a step function. However, the experimental tests show that the applied load has not a constant value immediately after imposing and it takes a short time to reach from zero to its maximum value. The interval time is called rising time. Different functions were defined here for load changes versus time. Based on them, DSIF at finite crack tip in an unbounded elastic body was obtained at a 2-D state of plane strain. In this research, the crack length was considered as limited with the length of 2a. The displacement fields were used for solving the wave equations. In the first function, loading time is imposed without limitation. In the second pulse, a pulse with a certain length that includes loading and unloading is applied. In this part, loading and unloading are considered as the linear and nonlinear functions. Finally, practical methods, which are effective at rising time, are presented. The main novelties of this study are:
1- Considering a more real load-time function rather than theoretical functions and solving
2- Calculating the stress filed around the crack using displacement filed instead of potential functions.

2 STATEMENT OF PROBLEM

As mentioned, in impact mechanics, a step function is used for defining impact load changes versus time. The function is defined as follows:

$$Heaviside\,(t\,) = \begin{cases} 0 & t \le 0 \\ 1 & t > 0 \end{cases} \qquad (1)$$

However, as shown in "Fig. 1", in real behaviour of structures and due to the inertial effects, the loading and unloading need a short time to reaches from zero to maximum (rising time) and return to zero (falling time).
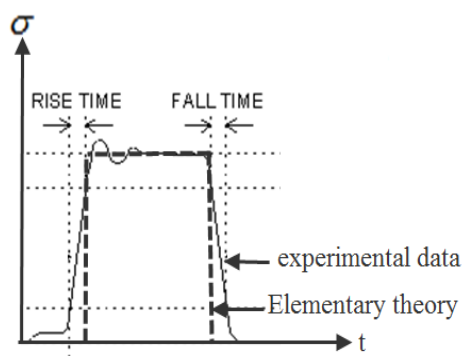
Fig. 1 Experimental and analytical comparison of real behavior of load changes versus time [19].

Therefore, including rising time value to examine a more real behaviour of materials is necessary for the equations. In this article, a mathematical function was defined in which load value is increasing in a linear manner so that the value reaches to its final value and remains at the same value after duration t*. In fact, this function is more similar to the real behaviour of material. Load changes versus time are defined as the following function (2).

$$\sigma(t) = \sigma^* \left[\frac{t}{t^*} H(t) - (\frac{t}{t^*} - 1)H(t - t^*) \right] \qquad (2)$$

Where, H is a step function, which is as "Eq. (3)":

$$H(t - t^*) = \begin{cases} 0 & t \le t^* \\ 1 & t > t^* \end{cases} \qquad (3)$$

Figure 2 shows diagram of load changes versus time and t* is the rising time.
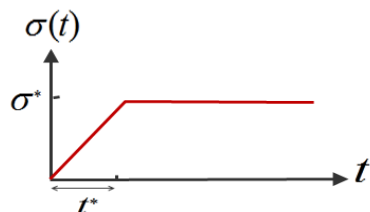
Fig. 2 Changes of impact load versus time [12].

Regarding "Eq. (2)" for load changes versus time, the equations related to DSIF at crack tip on an unbounded

plate will be calculated analytically. To calculate DSIF, assume a linear unbounded elastic body with a crack of length of 2a on it. It is assumed that in point y=0, the origin of coordinates is placed in the middle of the crack and the crack mouth is expanded to x direction. Figure 3 shows the parameters related to stress field around the crack.
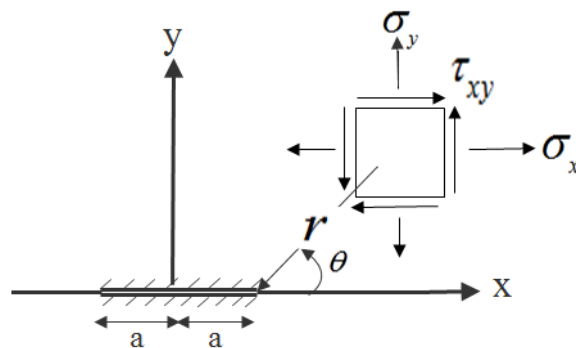
Fig. 3 Coordinates used for crack analysis.

An impact load, which is perpendicular to y=0 plate, is imposed on the crack surface at t=0 time. The load reaches to its maximum amount at t=t* time, i.e. σ^*, and remains during the whole period. As the load is applied perpendicularly, shear stress at the surface crack is equal to zero. Therefore, the effects of the second mode of fracture can be ignored and the calculations are only made based on the first mode of fracture. Regarding the symmetry of the problem and assuming x=0, boundary conditions in y=0 is as "Eq. (4)" [3]:

$$\tau_{xy}(x,0,t) = 0, \qquad |x| < \infty$$

$$\sigma_y(x,0,t) = \sigma_0 \left[\frac{t}{t^*} H(t) - (\frac{t}{t^*} - 1)H(t - t^*) \right]$$
$$, 0 \le |x| \le a \qquad (4)$$

$$v(x,0,t) = 0, \; |x| > 0$$

To solve the stress fields around the crack, two displacements functions of $u(x,y,t)$ and $v(x,y,t)$ are assumed, which both are true in the wave equation [7]. Therefore:

$$\frac{\partial^2 u(x,y,t)}{\partial x^2} + \frac{\partial^2 u(x,y,t)}{\partial y^2} = \frac{1}{C_p^2} \frac{\partial^2 u(x,y,t)}{\partial t^2}$$

$$\frac{\partial^2 v(x,y,t)}{\partial x^2} + \frac{\partial^2 v(x,y,t)}{\partial y^2} = \frac{1}{C_s^2} \frac{\partial^2 v(x,y,t)}{\partial t^2} \qquad (5)$$

In these equations, C_p is longitudinal wave speed, C_s is shear wave speed, u is displacement at x, and v is displacement in y direction. The relationship between stress and displacement fields is defined as follows:

$$\tau_{ij} = \lambda u_{k,k}\,\delta_{ij} + \mu(u_{i,j} + u_{j,i}) \tag{6}$$

Where:

$$\lambda = \frac{\nu E}{(1+\nu)(1-2\nu)} \qquad\qquad \mu = \frac{E}{2(1+\nu)}$$

$$C_p = \left(\frac{\lambda+2\mu}{\rho}\right)^{\frac{1}{2}} \qquad\qquad C_s = \left(\frac{\mu}{\rho}\right)^{\frac{1}{2}}$$

Consequently:

$$\sigma_{yy} = (2\mu+\lambda)\frac{\partial v}{\partial y} + \lambda(\frac{\partial u}{\partial x})$$
$$\tau_{xy} = \mu(\frac{\partial u}{\partial y} + \frac{\partial v}{\partial x}) \tag{7}$$

As the analytical solution is difficult in a time-place environment, to solve them, they are first taken to Laplace environment. Then, with respect to the geometrical symmetry, the Fourier sine and cosine transform are used for solving the problems. To do so, Laplace displacement is defined as follows [20]:

$$\bar{f}(s) = \int_0^\infty f(t)e^{-st}dt$$
$$f(t) = \frac{1}{2\pi i}\int_{Br} \bar{f}(s)e^{st}dt \tag{8}$$

Now, Laplace is taken of "Eq. (5)" versus time consequently:

$$\frac{\partial^2 \bar{u}(x,y,s)}{\partial x^2} + \frac{\partial^2 \bar{u}(x,y,s)}{\partial y^2} = \frac{s^2}{C_p^2}\bar{u}(x,y,s)$$
$$\frac{\partial^2 \bar{v}(x,y,s)}{\partial x^2} + \frac{\partial^2 \bar{v}(x,y,s)}{\partial y^2} = \frac{s^2}{C_s^2}\bar{v}(x,y,s) \tag{9}$$

Now, the Fourier sine and cosine transform, which are defined as "Eq. (10)", are used for transforming "Eq. (9)" into an ordinary differential equation [20]:

$$F(p) = \int_0^\infty f(x)\sin(px)dx$$
$$f(x) = \frac{2}{\pi}\int_0^\infty F(p)\sin(px)dp \tag{10-a}$$

$$F(p) = \int_0^\infty f(x)\cos(px)dx$$
$$f(x) = \frac{2}{\pi}\int_0^\infty F(p)\cos(px)dp \tag{10-b}$$

By applying the transforms of Eq. (10) in Eq. (9), we have:

$$-p^2 U(p,y,s) + \frac{\partial^2 U(p,y,s)}{\partial y^2} = \frac{s^2}{C_p^2}U(p,y,s)$$
$$-p^2 V(p,y,s) + \frac{\partial^2 V(p,y,s)}{\partial y^2} = \frac{s^2}{C_s^2}V(p,y,s) \tag{11}$$

Which are two ordinary differential equations and their general solution are as "Eq. (12)":

$$U(p,y,s) = A(p,s)e^{-\gamma_1 y} + A_1(p,s)e^{\gamma_1 y}$$
$$V(p,y,s) = B(p,s)e^{-\gamma_2 y} + B_1(p,s)e^{\gamma_2 y} \tag{12}$$

Where, $\gamma_1 = \left(p^2 + \frac{s^2}{C_p^2}\right)^{\frac{1}{2}}$, $\gamma_2 = \left(p^2 + \frac{s^2}{C_s^2}\right)^{\frac{1}{2}}$ and

$A_1(p,s)$ and $B_1(p,s)$ are vanished because when y tends to infinity, displacement value cannot be infinite. By taking reverse integration of "Eq. (12)", we have:

$$\bar{u}(x,y,s) = \int_0^\infty A(p,s)e^{-\gamma_1 y}\sin(px)dp \tag{13-a}$$

$$\bar{v}(x,y,s) = \int_0^\infty B(p,s)e^{-\gamma_2 y}\cos(px)dp \tag{13-b}$$

Now, we have two equations based on x, y and p. To apply the effects of boundary conditions, first, Laplace transform is applied to them. Therefore:

$$\bar{\sigma}_{yy}(x,y,p) = (2\mu+\lambda)\frac{\partial \bar{v}}{\partial y} + \lambda(\frac{\partial \bar{u}}{\partial x}) \tag{14-a}$$

$$\bar{\tau}_{xy}(x,y,p) = \mu(\frac{\partial \bar{u}}{\partial y} + \frac{\partial \bar{v}}{\partial x}) \tag{14-b}$$

$$\bar{\tau}_{xy}(x,0,p) = 0, \qquad |x| < \infty \tag{15-a}$$

$$\bar{\sigma}_y(x,0,p) = \sigma_0\frac{1-e^{-st^*}}{t^* s^2}, \qquad 0 \le |x| \le a \tag{15-b}$$

$$\bar{v}(x,0,t) = 0, \ |x| > 0 \tag{15-c}$$

By replacing equations (13-a) and (13-b) in "Eq. (14-b)" and applying boundary conditions (15) and inserting y=0, we have:

$$\bar{\tau}_{xy}\Big|_{y=0} = \int_0^\infty \left[\gamma_1 A(p,s) - pB(p,s)\right]\sin(px)dp = 0$$

$$\Rightarrow B(p,s) = D(p,s) \tag{16}$$

$$A(p,s) = \frac{p}{\gamma_1} D(p,s)$$

Now, by replacing equations (13-a) and (13-b) in "Eq. (14-a)" and applying "Eq. (15)" boundary conditions and inserting y=0:

$$\bar{\sigma}_y\Big|_{y=0} = \int_0^\infty pF(p,s)D(p,s)\cos(px)dp$$

$$= \sigma_0 \frac{1-e^{st^*}}{t^*s^2} \tag{17}$$

$$where \ F(p,s) = \left[(2\mu+\lambda)\frac{\gamma_2}{p} + \lambda\frac{p}{\gamma_1}\right]$$

Meanwhile, with respect to the boundary conditions 15-c, we have:

$$\bar{v}\Big|_{y=0} = \int_0^\infty D(p,s)\cos(px)dp = 0 \tag{18}$$

As a result, a dual integral equation is obtained, which is defined as follows:

$$\begin{cases} \int_0^\infty pF(p,s)D(p,s)\cos(px)dp = \sigma_0 \frac{1-e^{st^*}}{t^*s^2} & \text{(19-a)} \\ \int_0^\infty D(p,s)\cos(px)dp = 0 & \text{(19-b)} \end{cases}$$

To solve the above dual integral equation, we assume that [7]:

$$D(p,s) = \int_0^a \varphi(\tau,s)J_0(p\tau)d\tau \tag{20}$$

Moreover, two properties of Integral equation that are shown in equations (21) and (22) are used [21].

$$f(x) = \int_a^x \frac{g(\tau)d\tau}{(x^2-\tau^2)^\zeta}, \qquad 0 < \zeta < 1$$

$$g(x) = \frac{2\sin(\pi\zeta)}{\pi}\frac{d}{dx}\int_a^x \frac{\tau f(\tau)d\tau}{(x^2-\tau^2)^{1-\zeta}} \tag{21}$$

$$\int_0^\infty \cos(px)J_0(p\tau)d\tau = \begin{cases} \dfrac{1}{\sqrt{t^2-x^2}}, & x < \tau \\ 0, & x > \tau \end{cases} \tag{22}$$

By replacing "Eq. (20) in Eq. (19-a)" and using equations (21) and (22), we have:

$$\varphi(\tau,s) + \int_0^a \varphi(\theta,s)K(\theta,s)d\theta = -\sigma_0\tau(\frac{1-e^{st^*}}{t^*s^2})$$

$$K(\theta,s) = \tau\int_0^\infty p(F(p,s)-1)J_0(p\tau)J_0(p\theta)dp \tag{23}$$

To solve the above equation, $\varphi(\theta,s)$ value should be calculated. By putting this value in "Eq. (23)" and calculating $\varphi(\tau,s)$ and finally replacing it in Eq. (20) and the result in "Eq. (17)", $\bar{\sigma}_y$ value is obtained.

Meanwhile, for $r = x-a, r \ll a$ dynamic stress intensity factor in a Laplace environment and $\bar{\sigma}_y$ stress value are as "Eq. (24)" [7]:

$$\bar{\sigma}_y = \frac{\bar{K}_1(s)}{\sqrt{2r}} \tag{24}$$

Where, r is the point very close to crack tip. Therefore:

$$\bar{K}_1 = \frac{\phi(a)}{\sqrt{a}} \tag{25}$$

To solve "Eq. (23)", first, the equation is non-dimensionalized by changing the following variables.

$$\tau = ar, \qquad \theta = a\rho, \qquad \delta = ap \tag{26}$$

As a result:

$$\phi(t) = \phi(ar) = -\sigma_0 ar^{\frac{1}{2}}\Phi(r)\frac{1-e^{st^*}}{t^*s^2}$$

$$\Phi(r,s) + \int_0^1 \Phi(\rho,s)L(a\rho,ar)d\rho = r^{\frac{1}{2}} \tag{27}$$

$$L(a\rho,ar) = (r\rho)^{\frac{1}{2}}\int_0^\infty \delta\left[F(\delta/a,s)-1\right]J_0(\delta r)J_0(\delta\rho)d\delta$$

After solving the above equation and replacing it in "Eq. (25)", we have:

$$\bar{K}_1(s) = -\sigma_0 a^{\frac{1}{2}}\Phi(1,s)\frac{1-e^{st^*}}{t^*s^2} \tag{28}$$

The dynamic stress intensity factor in a Laplace space will be obtained using this relation. To calculate this factor in a space-time environment, it is necessary to apply the reversed Laplace transform as follows:

$$K_1(t) = \frac{\sigma_0 a^{\frac{1}{2}}}{2\pi i} \int_{Br} \Phi(1,s) \frac{1-e^{st^*}}{t^* s^2} e^{st} ds \qquad (29)$$

The numerical method and software MATLAB code are used for calculating "Eq. (29)". The numerical method used for solving this equation is presented in References [22-23]. By calculating $\Phi(1,s)$ and replacing it in "Eq. (29)", the DSIF is calculated. The above method is also used for a limited-time pulse shown in "Fig. 4", The relation between parameters of this pulse is presented in "Eq. (30)".
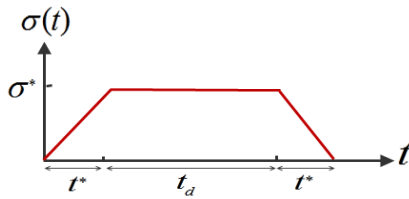
Fig. 4   Changes of impact load versus time for a finite pulse [12].

$$\sigma(t) = \sigma_0 \left\{ \begin{array}{l} \frac{t}{t^*}\left[H(t)-H(t-t^*)\right]+ \\ \left[H(t-t^*)-H(t-t^*-t_d)\right] \\ +\left(2-\frac{t-t_d}{t^*}\right)\times \\ \left[H(t-t^*-t_d)-H(t-2t^*-t_d)\right] \end{array} \right\} \qquad (30)$$

The calculation method is not mentioned here due to the large volume of calculations.

$$K_1(t) = \frac{\sigma_0 a^{\frac{1}{2}}}{2\pi i} \times$$
$$\int_{Br} \Phi(1,s)(\frac{1-e^{-st^*}-e^{-s(t^*+t_d)}+e^{-s(2t^*+t_d)}}{t^* s^2})e^{st} ds \qquad (31)$$

"Eq. (31)" can also be solved using the above method. It is completely clear from this equation, that if the pulse duration tends to infinity ($t_d \to \infty$), the "Eq. (31)" converts to the "Eq. (29)". To extract the results, a nonlinear function is selected for load changes in rising and falling times. This function is shown in "Eq. (32)". The chart of this loading changes vs. time is shown in "Fig. 5" for n=2, n=0.5. It is obvious that for n=1 the changes of loading and unloading are linear and similar to the "Fig. 4".

$$\sigma(t) = \sigma_0 \left\{ \begin{array}{l} (\frac{t}{t^*})^n\left[H(t)-H(t-t^*)\right] \\ +\left[H(t-t^*)-H(t-t^*-t_d)\right] \\ +\left(2-\frac{t-t_d}{t^*}\right)^n \times \\ \left[H(t-t^*-t_d)-H(t-2t^*-t_d)\right] \end{array} \right\} \qquad (32)$$
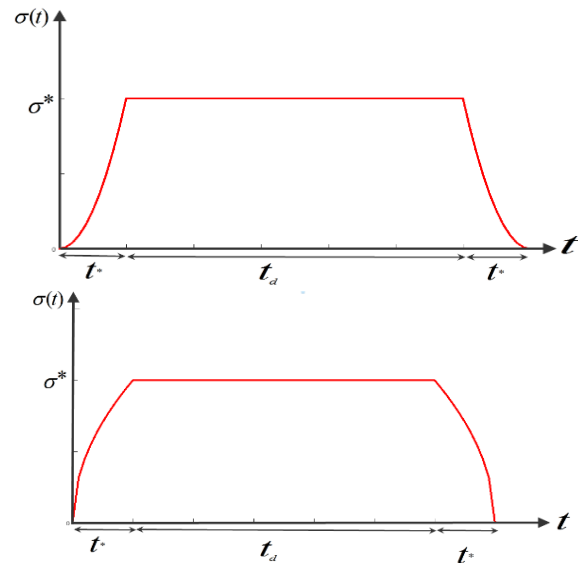
Fig. 5   Changes of impact load versus time for n=2(left) and n=0.5(right).

For different values of n, DSIF can be calculated from "Eq. (33)".

$$K_1(t) = \frac{\sigma_0 a^{\frac{1}{2}}}{2\pi i} \times$$
$$\int_{Br} \Phi(1,s) \left(\begin{array}{l} \dfrac{\Gamma(n+1)}{t^{*n} s^{n+1}} - \dfrac{e^{-s}\mathscr{L}\left[(t+1)^n\right]}{t^{*n}} + \\[2mm] \dfrac{e^{-t^*s}+e^{-(t^*+t_d)s}}{s} + \\[2mm] \left(\dfrac{-1}{t^*}\right)^n \left(\begin{array}{l} e^{-(t^*+t_d)s} \times \\ \mathscr{L}\left[(t-t^*+2t_d)^n\right] \\ -e^{-(2t^*+t_d)s} \times \\ \mathscr{L}\left[(t+2t_d)^n\right] \end{array} \right) \end{array} \right) ds \qquad (33)$$

3   DISCUSSION

As mentioned later, in real behaviour of materials, immediately after applying an impact load, its amount does not reach the final level and it takes a while for the load to impose completely. To study the accuracy of the obtained results, the equations are solved and drawn in this section. Then the effects of rising time and pulse shape on DSIF are discussed. To do so, an infinite plate that containing a central crack with length 10 cm is assumed. The sample is made of steel. The mechanical properties are mentioned in "Table 1", so that we could compare the results with other references.

To verify the accuracy of "Eq. (29)", a pulse with different rising time is applied and the changes of DSIF vs. time are presented in "Fig. 6". As it can be seen in "Fig. 6", when t* tends to zero ($t^* \rightarrow 0$), the results are matched with the results of Heaviside function in reference 3. By increasing the rising time, the effects of inertia and DSIF reduced.

Table 1 Mechanical properties of the material under study

	Density (kg/m3)	Elasticity Module (GPa)	Poisson's ratio	λ (GPa)	μ (GPa)	C_1 (m/s)	C_2 (m/s)
Steel	7800	200	0.3	115.4	76.9	5875	3140
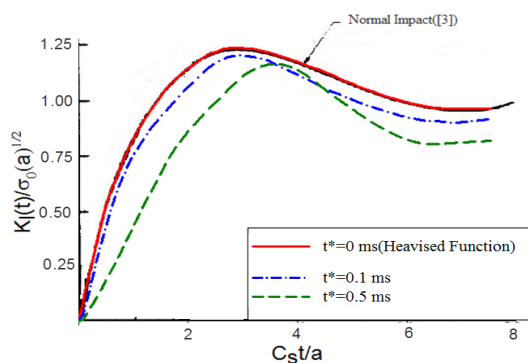
Fig. 6   Effect of rising time in dynamic stress intensity factor.

In experimental tests, changing the rising time duration was performed by putting an interface pad between cracked samples and impacting object. As far as yield stress is concerned, the interface sample should be softer than the one of the cracked objects. As far as stiffness is concerned, the stiffness of interface sample should be lower than the one of the cracked objects [24-26]. In fact, at the time of applying impact load, the softer material by increasing the applied rising time decreases dynamic stress intensity factor, which is followed by reducing fracture probability. For tensile loads, it can be done by putting a Springer. In fact, after imposing an impact load, springs prevent sudden increase of the load and create a delay in rising time. In fact, this result satisfies the aim of the present article that is reduction of the amount of DSIF.

Next, a pulse with limited time duration that contain loading and unloading is applied to cracked media and DSIF is shown in "Figs. 7 & 8". In "Fig. 7", the rising time is 0.1 Ms and in Fig. 8, the rising time is 0.5 Ms, but the pulse time duration is different. As it can be seen in these figures, when the pulse duration is too limited, the DSIF cannot reaches to its maximum value. In this situation, because of the inertia effects, before the DSIF reaches to its maximum value, the unloading is started and so it never starts decreasing.
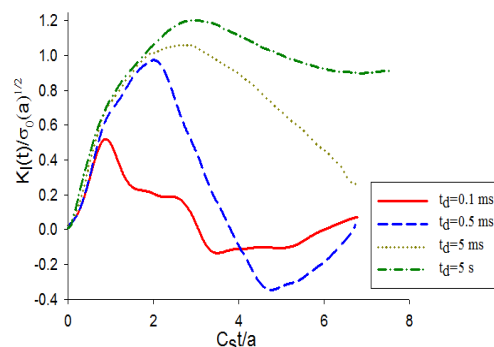
Fig. 7   Effect of pulse duration in DSIF for t*=0.1 Ms.
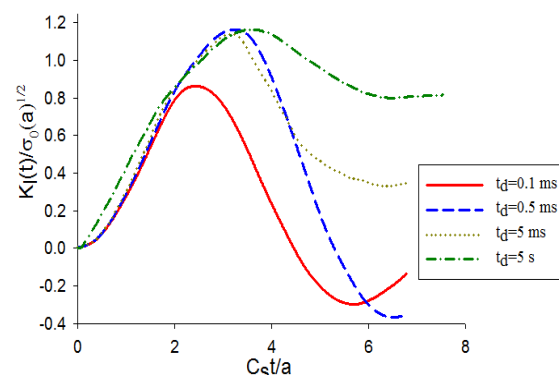
Fig. 8   Effect of pulse duration in DSIF for t*=0.5 Ms.

Then, it is considered that the changes of loading and unloading is non-linear. The function of variation is

assumed as a power function. For n=2 and n=0.5 in this relation, DSIF is calculated from "Eq. (33)". These results are compared with linear results from last part for long td in "Figs. 9 & 10". Results show that the maximum of DSIF is independent of loading condition and final value of it is similar for n=1 (linear) and n=2 or n=0.5 (nonlinear).
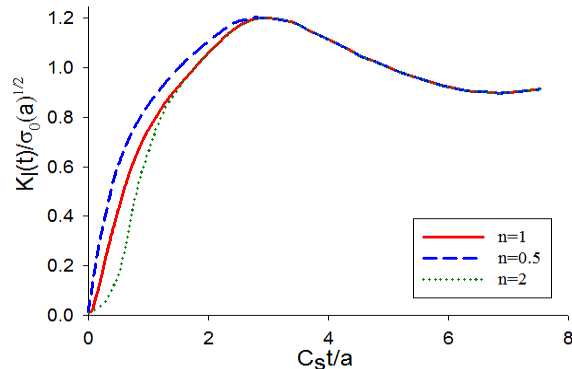
Fig. 9   Effect of linearity and non-linearity of loading on DSIF for t*=0.1 Ms.
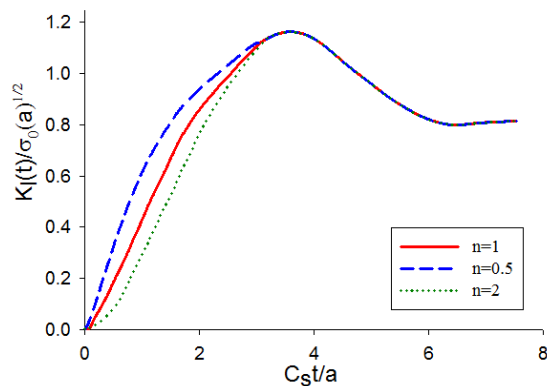
Fig. 10   Effect of linearity and non-linearity of loading on DSIF for t*=0.5 Ms.

5   CONCLUSIONS

Analytical solution of shape and rising time of pulse effect on DSIF were discussed in the present article. It was observed that with the rise-time increasing, DSIF decreases. These phenomena are occurred because of inertia effects. In impact pulses with limited duration, the results are a little different. In these cases, for low time duration, the DSIF cannot reach to the maximum value, but for pulses with a sufficient loading time duration, the DSIF increased. In addition, results show that the linearity or non-linearity of loading have no effects of DSIF maximum value but it changes the variation of DSIF vs. time.

REFERENCES

[1]   Sih, G. C., Elastodynamic Crack Problems, Noordhoff International Publishing, Company bv Leyden, Netherland, 1977, pp. 1-23.

[2]   Freund, L. B., Dynamic Fracture Mechanics, Cambridge University press, New York, 1998, pp. 52-82

[3]   Sih, G. C., Embley, G. T., and Ravera, R. S., Impact Response of a Finite Crack in Plane Extension, International Journal of Solids and Structures, Vol. 8, No. 7, 1972, pp. 977-993.

[4]   Thau, S. A., Tsin-Hwei, L., Transient Stress Intensity Factors for A Finite Crack in an Elastic Solid Caused by A Dilatational Wave, International Journal of Solids and Structures, Vol. 7, No. 7, 1971, pp. 731-750.

[5]   Ing, Y. S., Ma, C. C., Transient Response of a Finite Crack Subjected to Dynamic Anti-Plane Loading, International journal of fracture, Vol. 82, No. 4, 1996, pp. 345-362.

[6]   Ing, Y. S., Ma, C. C., Exact Transient Full–Field Analysis of a Finite Crack Subjected to Dynamic Anti–Plane Concentrated Loadings in Anisotropic Materials, Proceedings of the Royal Society A: Mathematical, Physical and Engineering Sciences, Vol. 461, No. 2054, 2005, pp. 509-539.

[7]   Kassir, M., Bandyopadhyay, K., Impact Response of a Cracked Orthotropic Medium, Journal of applied mechanics, Vol. 50, No. 3, 1983, pp. 630-636.

[8]   Rubio-Gonzalez, C., Mason, J., Dynamic Stress Intensity Factor Due to Concentrated Loads On a Propagating Semi-Infinite Crack in Orthotropic Materials, International journal of fracture, Vol. 118, No. 1, 2002, pp. 77-96.

[9]   Rodríguez-Castellanos, A., Rodríguez-Sánchez, J., Núñez-Farfán, J., and Olivera-Villaseñor, R., Crack Effects On the Propagation of Elastic Waves in Structural Elements, Revista mexicana de física, Vol. 52, No. 2, 2006, pp. 104-110.

[10]   Itou, S., Dynamic Stress Intensity Factors Around a Cylindrical Crack in an Infinite Elastic Medium Subject to Impact Load, International Journal of Solids and Structures, Vol. 44, No. 22-23, 2007, pp. 7340-7356.

[11]   Eslami, S., Amini, F, Dynamic Stress Intensity Factors Due to Scattering of Harmonic Waves by A Crack in an Infinite Medium, Fatigue & Fracture of Engineering Materials & Structures, Vol. 31, No. 10, 2008, pp. 918-927.

[12]   Zhang, C., Gross, D., On Wave Propagation in Elastic Solids with Cracks, Computational Mechanics Publications, 1998, pp. 45-59.

[13]   Chirino, F., Dominguez, J., Dynamic Analysis of Cracks Using Boundary Element Method, Engineering Fracture Mechanics, Vol. 34, No. 5-6, 1989, pp. 1051-1061.

[14]   Fedelinski, P., Aliabadi, M., and Rooke, D., The Dual Boundary Element Method in Dynamic Fracture

Mechanics, Engineering Analysis with Boundary Elements, Vol. 12, No. 3, 1993, pp. 203-210.

[15] Phan, A.V., Gray, L. J., and Salvadori, A., Transient Analysis of the Dynamic Stress Intensity Factors Using Sgbem for Frequency-Domain Elastodynamics, Computer Methods in Applied Mechanics and Engineering, Vol. 199, No. 45-48, 2010, pp. 3039-3050.

[16] Ebrahimi, S., Phan, A.V., Dynamic Analysis of Cracks Using the Sgbem for Elastodynamics in The Laplace-Space Frequency Domain, Engineering Analysis with Boundary Elements, Vol. 37, No. 11, 2013, pp. 1378-1391.

[17] Malezhik, M., Malezhik, O., and Chernyshenko, I., Photoelastic Determination of Dynamic Crack-Tip Stresses in an Anisotropic Plate, International Applied Mechanics, Vol. 42, No. 5, 2006, pp. 574-581.

[18] K. Ravi-Chandar, Dynamic Fracture, Elsevier, 2004, pp. 9-46.

[19] Wang, L., Foundations of Stress Waves, Amsterdam, Netherland, 2011, pp. 57-87.

[20] Dyke, P. P., An Introduction to Laplace Transforms and Fourier Series, 2nd ed, Springer, New York, 2014, pp. 129-152.

[21] Erdelyi. A., Sneddon, I. N., Fractional Integration and Dual Integral Equations, Canadian Journal of Mathematics, Vol. 14, No. 1, 1962, pp. 685-693.

[22] Miller, M. K., Guy, W.T., Numerical Inversion of the Laplace Transform by Use of Jacobi Polynomials, SIAM Journal on Numerical Analysis, Vol. 3, No. 4, 1966, pp. 624-635.

[23] Sneddon, I. N., Mixed Boundary Value Problems in Potential Theory, New York: Wiley, 1966, pp. 69-85.

[24] Ramírez, H., Rubio-Gonzalez, C., Finite-Element Simulation of Wave Propagation and Dispersion in Hopkinson Bar Test, Materials & design, Vol. 27, No. 1, 2006, pp. 36-44.

[25] Elkaranshawy, H. A., Bajaba, N. S., A Finite Element Simulation of Longitudinal Impact Waves in Elastic Rods, Materials with Complex Behaviour II, Vol. 16, No. 1, 2012, pp. 3-17.

[26] Lu, Y., Li, Q., Appraisal of Pulse-Shaping Technique in Split Hopkinson Pressure Bar Tests for Brittle Materials, International Journal of Protective Structures, Vol. 1, No. 3, 2010, pp. 363-390.